The Effect Of Dopant And Glass Composition On Judd-Ofelt Parameters And Radiative Decay Rate Of Erbium Doped Zinc Borate Glasses For Broad Band 1.53 µm Emission

D. Vijaya Sri, S. Hima Bindu, Ch. Linga Raju

Abstract: Erbium doped zinc borate glass system containing constant concentrations of M^{2+} oxides with the molar percentage of 10MO-(30-x)ZnO-$60B_2O_3$-(x)Er_2O_3 (where M = Ca, Sr & Ba and x=1, 2 & 3 mol %) were synthesized and characterized using various techniques like XRD, FTIR, optical absorption, photo-luminescence and decay curve analysis. The absorption spectra specified the ionic nature of the organized Er^{3+}: MZB glass. The high spectral intensity values (*f*) for the transitions $^4I_{15/2}\rightarrow{}^2H_{11/2}$ and $^4I_{15/2}\rightarrow{}^4G_{11/2}$ reveal the high site asymmetry around Er^{3+} ions. Broad & intense 1.53 µm infrared fluorescence for the transition $^4I_{13/2}\rightarrow{}^4I_{15/2}$ is observed at 379 nm. The green emissions in photo-luminescence spectra for $^4I_{13/2}\rightarrow{}^4I_{15/2}$ transition indicate strong quenching. The values of bandwidth (292 nm), stimulated cross section (5.3 cm^2) and lifetime (1.65 ms) along with broad emission of $^4I_{13/2}$ level in Er^{3+}: MZB glasses suggest the present prepared glass system be potential beneficial candidate for high gain broad band amplifiers in WDM systems.

Key words: Erbium doped MZB glasses, FTIR characterization, Optical studies, J-O intensity parameters, Rare earth Luminescence, Decay analysis.

1. Introduction

Over the recent past, tremendous research work has been accomplished on the research of luminescent properties of lanthanide ion doped glasses towards the development of infrared lasers and broad amplifiers in telecommunication industry [1]. The glass network are strongly influenced by the local structure occupied by the RE ions [2]. These properties of the Er^{3+} ions were examined in various crystalline and non-crystalline matrices to explore their applicability to achieve lasers in the near infrared vicinity [3-5]. Dopants can firmly impact optical behavior. The current research is progressing towards the optical characteristics of the Er^{3+} ions because of the transition $^4I_{13/2}\rightarrow{}^4I_{15/2}$ at around the wavelength 1535 nm, which is best for the optical data transmission applications [6]. The optical gain enhanced up to a specific point with Er^{3+} ion concentration and after that have a tendency to form a group, which modifies the local sites and the optical properties of the glass network. Finally, the host matrix becomes optically inactive [7]. The rare earth ions act as prominent luminescent materials because of their sharp and intense emission spectra due to their 4f intra shell transitions. The green emission at around 605 nm corresponding to $^4I_{13/2}\rightarrow{}^4I_{15/2}$ transition will be useful for the development of an efficient broad band optical device as a way to be utilized in wavelength-division-multiplexing system frame works and green laser applications [8].

The base matrix composition plays a vital role in determining the characteristics of a glass. Recently significant interest has been taken in adding two or more glass modifiers in the composition for different scientific and technological applications [6]. Over the years, binary alkali earth borate glasses 10MO-30ZnO-$60B_2O_3$ (M^+, alkaline earth metal ion) have been extensively studied to make clear their structure, i.e. the nature and relative population of the borate units building the glass network. These are helpful in understanding the structural origin of the nonmonotonic variation of physical properties with alkaline earth oxide content, generally known as the 'boron anomaly'. Alkaline earth ions (Ca^{2+},Sr^{2+},Ba^{2+}) behave like alkali modifier ions at low MO contents and the fraction of four coordinated boron atoms follows the x/(1-x) law as in alkali borates. Indeed, the composition dependence of this fraction in the barium borate system was found to be very similar to that in the lithium and sodium borate glasses [9]. These oxides may also cause a change in oxygen coordination number from two to three apart from their glass modifying or forming properties. This was reported in SrO–B_2O_3 glasses [10]. Likewise, M^{2+} oxides improve the glass forming nature. Because of these properties, it has numerous applications in solid state devices, electro chemical, electro and electric optical devices [11]. Transition metal ions are generally carried out as probes in glasses to give valuable information about electronic states and local structures with the aid of spectroscopic techniques [12]. Zinc Oxide, an II-VI compound semiconductor with a huge band gap of about 3.4 eV and a large substantial binding energy (~60 meV), is a prominent material in optical devices which include blue, violet & UV-LEDs and LDs (Laser Diodes) [13]. Due to its low melting point, they have been used as good sintering agent. The best transparency in a mid infrared region, lowest phonon energy (~550cm^{-1}) and high refractive index (~2.3) of heavy metal oxides are best for photonics and optical communication network [14]. Borate is an appropriate optical material as it is having more transparency, low melting point, high thermal stability and good solubility [15].

- *D.Vijaya Sri is currently pursuing Doctoral Degree program in Physics in Acharya Nagarjuna University, Andra Pradesh, India and faculty in Physics in T.R.R.Government Degree College Kandukur. E-mail: devarakondakoppula@gmail.com*
- *Dr.Ch.Linga Raju, Associate Professor, Research Guide, Acharya Nagarjuna University, Andra Pradesh, India. E-mail: drchlraj@yahoo.com*

The significant feature of borate glass is that it shows variations in its structural properties when alkaline earth cations are brought inside the glass matrix [16]. The addition of alkaline oxides modifies the random network of boroxal rings of pure B_2O_3 into four coordinate borate atoms [17]. Balaji Rao et al., 2008 [18], specified the result of incorporation of alkaline earth ions in the borate host. He distinguished that the trigonal and the tetrahedral states are significantly attributed to the creation of ionic bond with oxygen atom. The modified borate structure has an amorphous nature and all states have large phonon energy. This large phonon energy (~1400 cm^{-1}) [19] of borate glass may be avoided by choosing suitable network modifying and forming cations which include ZnO and alkaline earth ions in borate community. Alkaline earth borate glasses with transition-metal ions show specific ionic conduction [20], optical absorption [21] and can act as an efficient solid electrolyte in batteries. Due to excellent optical, electrical and thermal properties of MZB glasses, they are preferred in microelectronics, optics and fiber optics [2]. To get efficient and stable emission in a particular spectral range, doping of ZnO materials with lanthanides has been proposed. Rare earth ions require the coordination of a sufficiently more number of non-bridging oxygen ions. Zinc oxide as network modifier breaks bridging oxygen ions to form non-bridging oxygen ions and can be utilized to make possible the incorporation of rare earth ions because of their bigger size compared with that of a basic network. So rare earth ion doped ZnO has the potential to be a highly multifunctional material with coexisting semiconducting, electromechanical and optical properties [22]. The present work reviews about the effect of alkaline earth ions and the concentration of Ln^{3+} ions on structural, optical and luminescence properties of Er^{3+}: MZB glasses with powder X-ray diffraction, FTIR, optical absorption, emission and fluorescence life time, in conjuction with J-O parameters as a characteristic of different compositions of alkaline earth ions and erbium concentrations in the host matrix.

2. Experimental

2.1. Sample synthesis

The present system 10MO-(30-x)ZnO-60B_2O_3-(x)Er^{3+} (where M=Ca,Sr&Ba and x=1,2,3 mol %) with molar composition as shown in the Table 1, are synthesized through the melt quenching approach. Using the batches of 10gm of stoichiometric ratio of compounds, the glasses were prepared as reported [6]. The samples were melted at 1150 ^{0}C for 45 min and then annealed at 400 ^{0}C for 4h.The prepared glasses are light pink in shade and it has become dark pink by the increasing concentration of the erbium ion. Finally the polished glass is used study the physical and optical properties. (Hereafter erbium doped alkaline earth zinc borate glasses are referred as Er^{3+}: MZB and Calcium Zinc Borate, Barium Zinc Borate and Strontium Zinc Borate as CZB, BZB, and SZB respectively).

2.2. Material characterization

Density was measured by the Archimedes's method utilizing xylene as an immersion liquid. The FTIR spectra of Er^{3+}: MZB glasses have been recorded within the range 4000-400 cm^{-1} by employing KBr pellet technique using JASCO FTIR 6200 spectrometer to understand the structural nature of vitreous systems. Optical absorption spectra had been recorded using JASCO V-270 spectrophotometer to study the optical behavior in the range 250-1700 nm. Excitation and Emission spectra were recorded on the HITACHI 650-10s fluorescence spectrophotometer at room temperature to know the luminescence properties.

3. Results and discussion

3.1. Physical properties

The atomic structure and conduction mechanism of the glass matrix is known from its physical properties. The concentration of the Ln^{3+} ions in the glass lattice influences the laser gain of the host material [23]. Various physical properties of the Er^{3+}: MZB glass samples were summarized in the Table 2. Density is estimated to determine the abrupt modifications that are occurred in the glass network with the introduction of erbium ion. From Table 2, density is gradually decreased with the high concentration of Er^{3+} in the glass network at the rate of zinc oxide. This is due to the formation of NBO (non bridging oxygen) atoms, results the increase of free spatial distances and rare earth ion grouping in the system [24]. The increasing trend of the refractive index with erbium results enhancement of ionic refractivity of non-bridging oxygen, when zinc was compensated with erbium ion. The parameter molar volume pertains to distribution of oxygen in the glass community [25], which increases with the erbium ion concentration attributed to the increase of non bridging oxygen. The change in molar volume depends on the rate of change of both density and molecular weight [26]. Fig.1 specifies the change of density and refractive index with the erbium oxide content. The decrease of polaron radius (γ_p) with the increment of dopant ion concentration results strong field strength around Er^{3+} ions due to the decrease of average distance between Er-O ions [27]. Inter ionic distance for an erbium ion specifies expected decrease by the erbium content, which results the firmness of the glass system. The increase in molar polarizability with Er^{3+} ions is because of the extended range of the non bridging oxygen atoms that have higher polarizability than bridging oxygen atoms. It was also observed that the density is changed non-linearly with the replacement of alkaline earth content from Ca→Sr after that Sr→Ba in the glass framework at the cost of zinc oxide, due to the properties like dielectric relaxation, ionic diffusion, electrical conductivity and internal friction. The molar refraction expanded with the refractive index which in turn increases oxide ion polarizability and electronic polarizability. Metallization parameter values (M) had been observed to be much less than one which suggests the prepared system exhibit insulating nature [27].

3.2. Structural analysis

3.2.1. XRD studies

The X-ray patterns for undoped and Er^{3+} doped MZB glasses are shown in Fig.2. No sharp peaks within the pattern monitor the characteristic feature of amorphous material, indicating the glassy nature of the present system [29].

3.2.2. Analysis of FT- IR spectra

The FTIR spectrum of pure and Er^{3+}: MZB glasses are shown in Fig.3. Fourier transform infrared (FTIR) analysis was used to recognize the presence of functional groups and structural nature of vitreous systems. Addition of alkaline earth modifiers to the borate glass brings extreme changes in the structural units. Glasses in the strontium and calcium borate systems exhibit spectral characteristics intermediate to those of the Ba and Mg borate end members. The band assignments and interpretation of FTIR spectrum is quite complex due to the disordered nature of the vitreous systems and more variety of borate structural units with bridging & non-bridging oxygen ions [30]. The absorption bands for all sample glasses at around 425 cm^{-1} are because of ZnO tetrahedron [17, 31]. The weak band located at around 503 cm^{-1} corresponds to Er-O vibration [32].We consider the mid-infrared area (500–1600 cm^{-1}) where the vibrations of the boron oxygen structures are active in order to understand the impact of addition of M-O on the borate network structure. In pure borate glass, the 806 cm^{-1} frequency is a characteristic of boroxol ring. The vanishing of this band indicates the absence of boroxol groups ultimately it consists of BO_3 and BO_4 groups. These groups may be attached as random network in the prepared glass system [33]. The wide band focused at around 1265 cm^{-1} is assign to pyro borate groups [34], which is due to vibrations of boron atoms attached to non-bridging oxygen atoms in BO_4 units. The peaks at 2654, 2922 and 2854 cm^{-1} are attributed owing to hydrogen bonding and the broad absorption band at 3424 cm^{-1} is because of O-H stretching vibration. With the accumulation of dopant ions, O-H content decreases and will become invisible at higher RE concentrations. The minimum OH content in the glass enhances the optical attenuation and lowers quantum efficiency of the RE (Rare Earth) excited levels and also leads to luminescence quenching [35]. The creation of various borate units relies upon the modifier concentration. When the modifier ions are introduced in the network, these bands could get shifted basing on their cation effect [36]. From the spectrum, we observed the shifting of bands closer to higher wave number range with the mole percentage of erbium ion at an expense of zinc oxide.

3.3. Absorption studies

The absorption spectra of Er^{3+}: MZB glass in UV-VIS and NIR regions are shown in Fig.4. When rare earth ion is doped in the glass network, splitting of degenerated levels are observed due to the crystal field in the glass community. This results the inhomogeneous broadening in the glass. From Fig.4, many inhomogeneous bands from the ground state $^4I_{15/2}$ level to various excited levels, such as $^4I_{13/2}$, $^4I_{11/2}$, $^4F_{9/2}$, $^4S_{3/2}$, $^2H_{11/2}$, $^4F_{7/2}$, $^4F_{5/2}$, $^4F_{3/2}$, $^2G_{9/2}$, $^4G_{11/2}$, and $^4G_{9/2}$ corresponding to the energy positions at 1527, 975, 651, 541, 522, 487, 450, 441, 406, 378 and 365 nm respectively are found and are assigned basing on the reference [37]. Among those, $^4I_{15/2}\rightarrow{}^2H_{11/2}$ and $^4I_{15/2}\rightarrow{}^4G_{11/2}$ transitions show excessive intensity. There is no considerable shift in the band positions is seen due to the change in the chemical composition, however change in the intensity of the absorption bands is observed. But the strong absorption peak in NIR region at 975 nm, for $^4I_{11/2}$ level of Er^{3+} indicates that the glass can be excited efficiently by a 975 nm laser diode (LD).

3.3.1. Hypersensitive transitions

The transitions $^4I_{15/2}\rightarrow{}^2H_{11/2}$ and $^4I_{15/2}\rightarrow{}^4G_{11/2}$ in the UV-VIS vicinity, indicates high intensity among all the transitions and are referred as hypersensitive transitions, follows the selection rules $|\Delta S|=0$, $|\Delta L| \leq 2$ and $|\Delta J| \leq 2$ [38]. The positions and intensities of these transitions generally depend on the local surroundings of the rare earth ion, which in turn affects the significance of the intensity parameters. The oscillator strength value of these transitions indicates the higher asymmetry around dopant ions**.** The nephelauxetic ratio and bonding parameter are used for the identification of nature of the metal-ligand bond and are calculated with the help of absorption band positions. From the average values of β, the bonding parameter (δ) can be calculated. The bonding parameter (δ) values for Er^{3+}: MZB is given in the Table 4. The negative sign of δ indicates the ionic nature of the Er^{3+} ligand. According to the electro negativity concept [39], smaller the difference of electro negativity among cation and anion, stronger might be the covalence bond. The electro negativity values for Ca, Sr, Ba, Z, B, O & Er elements are 1, 0.95, 0.89, 1.6, 2.0, 3.4 & 1.24 respectively. The Er-O ligand is shows less covalent compare to ZnO content. The ionic nature of Er-O bond in MZB glasses goes on increasing, with the decrease of zinc concentration that is confirmed from the bonding parameter.

3.3.2. Optical band gap and Urbach energy

The optical band gap (E_g) is a critical parameter in the field of photonics, in expertise the electronic band structure of crystalline and non-crystalline materials. It is evaluated from the fundamental optical absorption edge in terms of direct and indirect allowed transitions [40]. By plotting $(\alpha h\upsilon)^2$ and $(\alpha h\upsilon)^{1/2}$ as a characteristic of photon energy $h\upsilon$, optical band gaps can be determined and are shown in Fig.5. The direct, indirect band gap values, Urbach energy and optical basicity values are calculated and are tabulated in the Table 3. The band gap values are observed to increase from 4.04 to 4.69 eV for every 1 mol % increase of erbium ion concentration and observed non-linear change 4.14, 3.98 & 4.32 eV for the change of alkaline earth ions one after the alternate from Ca, Sr & Ba, suggesting the growing of NBO content. Accordingly, localization states in the band gap are minimized. It causes an enrichment of the donor centers and shifts the absorption edge gradually towards higher energies. So, more electrons can easily be transferred from valance band to the conduction band [41]. Urbach energy (ΔE) is the measure of defect concentration. Materials with high Urbach values have a greater affinity to transform weak bands into defects [16]. From Table 3, we study that, the Urbach energy values decreasing from calcium to strontium and then increasing from strontium to barium. This suggests the structural disarray of the system. In the titled system, the lower structural disorder indicates the strong structural constancy of the system [42]. Fig.6 (a) shows the variation of band gap and Urbach energy with erbium ion concentration. The optical basicity (Δth**)** of an oxide glass medium specifies the potential to donate negative charges to the probe ion. It is predicted from its composition. From Fig.6 (b), the increasing of optical basicity with Er^{3+} ion means the increase of capability of oxide ions to transfer negative charge ions to the cations,

thereby results the increase of covalent nature among cation–oxygen bonding [43].

3.3.3. Oscillator strength

The oscillator strength (f) of an absorption transition of dopant ion inside the host matrix specifies the intensity of Ln^{3+} ion and dependence on the location below the absorption band [44]. The calculated oscillator strength (f_{cal}) of electric dipole transition from the initial ΨJ to the final $\Psi' J'$ state can be determined by the least square fit procedure. From f_{exp} values, the host dependent J-O intensity parameters (Ω_λ) and oscillator strengths f_{cal} for the electronic transitions have been assessed and tabulated in the Table 4. Good agreement has been noticed among f_{exp} and f_{cal} with small root mean square deviation (δ_{rms}) of 0.12 for SZB and 0.43, 0.72 for the replacement of strontium by calcium, barium respectively in the host matrix.

3.3.4. Judd-Ofelt analysis

The Judd–Ofelt theory enables to describe the transition intensities for different compositions. J-O parameters are essential to look at the local structure and bonding nature in the RE symmetry [44]. Also, these parameters along with emission measurements facilitate to evaluate different spectroscopic parameters that are essential to choose appropriate materials as hosts for Er^{3+} doped glasses. According to J-O hypothesis, the intensities of particular Ln^{3+} ion in the network are characterized by three parameters Ω_λ (λ=2, 4, 6). Among them, Ω_2 is very responsive to structural symmetry of Ln^{3+}ion site, the parameters Ω_4, Ω_6 identified with inflexibility of the network surrounding the Ln^{3+} ions [45]. Fig.7 demonstrates the variation of Ω_2 with erbium ion concentration. The intensity parameters follow the pattern $\Omega_2 > \Omega_6 > \Omega_4$, which are like similar to the other detailed glasses [8,46,47] and are tabulated in Table 5. The higher values of Ω_2 indicate the greater asymmetry of the ligand area closer to the rare earth ions. The increasing concentration of dopant ions at the cost of a network modifying cation (Zn) and changing the compound arrangement from Ca^{2+}, Sr^{2+} to Ba^{2+}, prompts an expansion in the symmetry across Er^{3+} ions and reduce of covalence factor among Er^{3+}- ligand bonds as the covalence between RE ion and ligand was related with the nearby cation field around the RE ion sites [45]. The same is also confirmed through its bonding parameter (δ). The higher rigidity of MZB glasses is confirmed by means of its higher Ω_6 values. The value of χ (spectroscopic quality factor) determines the present system is best for good laser activity [48].

3.4. Luminescence studies

To know the emission measurements of different erbium ion concentrations and the compositional effect in the host glass, luminescence spectrum was recorded by the exciting 379 nm wavelength. The luminescence efficiency mostly depends on the absorption intensity. Typically the PL peak shows asymmetric shape at ~1535 nm with overall features among 1400-1700 nm regions. This band is most essential for the applications in optical communication systems and IR laser applications. From Fig.8(a), we observed the intensity of broad emission band $I_{13/2} \rightarrow I_{15/2}$ at around 1.53 μm will increases with erbium ion concentration due to the non-radiative energy transfer among dopant ions resulting, luminescence quenching [49]. As a result, fluorescence intensity increases due to the increasing population of Er^{3+} ions at $I_{13/2}$ level, and also the peak at 1561 became shifted to 1558, 1543 nm. This broad emission band is best for optical communication applications [16]. However from Fig.8 (b), the intensity decreases with the change of alkaline earth metal ion from Ca to Sr and increases from Sr to Ba in the host matrix. The peak at 1530 nm was shifted to 1562 nm when Ba and Ca is replaced with Sr, indicates that the infrared luminescence is susceptible to a local environment across the origin of infrared luminescence. Among all the glasses, Er^{3+} doped calcium zinc borate glass showed higher emission intensity for 1535 nm emission band in the range of 1400–1700 nm useful for low loss communication window (S, C and L bands) [50]. The observed narrow peak towards the lower wave length side in Fig.8 (b) is governed by allowed magnetic dipole transition and independent of ligand field. But the broad band towards higher wavelength side is by forbidden electric dipole transition, which is dependent of ligand field, confirmed by the dominating J-O factor Ω_6 in the Table 5. Thus, the shape of bands reflects the trends in J-O parameters [51].

3.4.1. Radiative efficiencies

Radiative properties like radiative transitional probability (A), stimulated cross section (σ), branching ratio (β), gain band width (ΔG), radiative lifetime (τ) of the system were calculated using J-O parameters and are tabulated in Table 6& 7. In the present glass system, there exists only one emission band due to $^4I_{13/2} \rightarrow {}^4I_{15/2}$ transition (1530 nm) and the fluorescence branching ratio (β) for that is 1.00. The parameter σ_e (stimulated emission cross section) of a transition is important parameter for broad band amplifier applications. The values of σ_e and ΔG in the titled glass in Table 6 & 7 are suggestive for a less threshold and more gain optical amplifier applications [17].

3.5. Decay Analysis

Fig.9 specifies decay curves for the $^4I_{13/2}$ transition of Er^{3+}: MZB glasses. It shows single exponential behavior for all concentrations. Generally the lifetime of $^4I_{13/2}$ transition of Er^{3+} ion is strongly governed by radiative and non radiative processes. The variation of quantum efficiency (η) along with lifetimes of a host and dopant variation are listed in the Table 6. The experimental lifetime values corresponding to Er^{3+}: SZB (1,2,3 mol %) and for the host variation Er^{3+}: BZB & Er^{3+}: CZB (1 mol %) glasses are 1.77, 1.71, 1.65, 2.03 and 1.08 ms respectively. The values are compared with the other glasses PKSAEr [2], Tellurite [24], Er:NAP [42]. The decrease in lifetimes with an increase of erbium ion concentration is attributed to an increase in non radiative transition process like energy migration among Ln^{3+} ions followed by the transfer to luminescence quenching centers [52]. The experimental life time values (τ_m) are lower than the radiative life time values (τ_R). The quantum efficiency for $^4I_{13/2}$ level has been located to be 28-46 % for different compositions & concentrations of Er^{3+}: MZB glass. The gain band width for all prepared glasses are compared with the other reported glass systems like silicate [36], germinates [38] and phosphate [53]. These outcomes specify that glass system is of potential useful for WDM (wavelength division

multiplexing) optical network systems in the tele-communication applications.

4. Conclusions

From the physical and structural properties of erbium doped MZB glasses, we may conclude that,

- The non linear behavior with the change of M^{2+}ions in the host composition impacts the physical properties of the titled glass.
- The x-ray diffraction affirms the glassy nature of the glass system.
- FTIR analysis reveals the presence of BO_3 and BO_4 basic units in the network.
- The absorption spectra detailed the nature of the bond in Er^{3+}: MZB glasses.
- The J-O intensity parameters follow the pattern $\Omega_2 > \Omega_6 > \Omega_4$.
- The higher spectral intensity values (f) of the transition peaks $^4I_{15/2} \rightarrow {}^2H_{11/2}$ and $^4I_{15/2} \rightarrow {}^4G_{11/2}$ reveal the site asymmetry around Er^{3+} ion, also confirmed through the high value of Ω_2 (J-O parameter) and δ (bonding parameter).
- The decrement in χ (spectroscopic quality factor) determines the green emission quenching.
- The lower σ_e (stimulated emission cross section) and higher ΔG (gain bandwidth) values of the present glasses are best for near infrared optical amplifier applications.
- Er^{3+} doped calcium zinc borate glass showed higher emission intensity at 1535 nm emission band which was useful for low loss communication window.
- The consequences indicate that the E^{r3+} doped MZB glasses are best host materials for potential broad band amplifiers in the WDM system.

References:

[1]. D.V. R. Murthy, T. Sasikala, B. C. Jamalaiah, M. Jayasimhadri, Optical Communications, 284 (2011) 603-607.

[2]. D. E. Day, J. Non-Crystalline Solids, 21 (1976) 343-372.

[3]. S. Tanabe, Glass Sci.Technol, Glasstech. Bre., 74 (2001) 67.

[4]. S. Tanabe, C.R. Chim., 5 (2002) 815-824.

[5]. D. K. Sardar, C. C. Russell, R. M. Yow, J. Appl. Phys., 95 (2004) 1180.

[6]. K. Selvaraj, K. Marimuthu, J. Luminescence, 132 (2012) 1171-1178.

[7]. A. J. Kenyon, Progr. Quantum electron, 26 (2002) 225-284.

[8]. K. Linganna, M. Rathaiah, N. Vijaya, C. K. Jayasankar, V. Venkataramu, J. Ceramics International, 41 (2014) 5765-5771.

[9]. Greenblatt, S. & Bray, P. J. Phys. Chem. Glasses, 8 (5) (1967) 190-193.

[10]. Park, M. J. & Bray, P. J. Phys. Chem. Glasses, 13 (2) (1972) 50-62.

[11]. T. Ragavendra Rao, Ch. Venkata Reddy, R.V.S. S. N. Ravi Kumar, J. Non-Crystalline Solids, 357 (2011) 3373-3380.

[12]. G. Krishna Kumari, R.V.S.S.N. Ravi Kumar, Materials Research Bulletin, 47 (2012) 2646-2654.

[13]. Rita John, Rajaram Rajakumari, Nano-Micro Lett. 4 (2012) 65-72.

[14]. D. M. Shi, Q.Y. Zhang, J. Appl. Phys, 104 (2008) 123517-4.

[15]. O. Ravi, S. J. Dhoble, B. Ramesh, B. Deva Prasad Raju, J. Luminescence, 164 (2015) 154-159.

[16]. K. Selvaraju, N. Vijaya, K. Marimuttu, Phys. Status Solidi A, 210 (2013) 607- 615.

[17]. T. Ragavendra Rao, Ch. Venkata Reddy, R. V. S. S. N. Ravi Kumar, Materials Research Bulletin 46 (2011) 2222-2229.

[18]. R. Balaji Rao, A. Rosario, Materials Chemistry and Physics, 112 (2008) 186-197.

[19]. R. Reisfield, Spectroscopy of rare earth ions, in: A.Vaseashta, D.Dimova-Malinovska, J. M. Marshall, Nanostructured and advanced Materials, Springer (2005) 77-100.

[20]. M. Kim, H. W. Choi, C. H. Song, G. Y. Jin, Y. S. Yang, Solid State Ionics, 180 (2009) 527-530.

[21]. F. H. Elbatal,Y. M. Hamdy, S. Y. Marzouk, J. Non-Crystalline Solids 355 (2009) 2439- 2447.

[22]. Te Hua Fang, Walter water, J. Phys. Chem. Solids, 70 (2009) 1015-1018.

[23]. S. Mohan, K. S. Thindb, G. Sharmab, Brazilian Journal of Physics, 37 (2007) 1306-1313.

[24]. Zahar Ashur Said Mahraz, M.R. Sahar, S. K. Ghoshal, M. Reza Dousti, J. Luminescence, 144 (2013) 139-145.

[25]. Yahya, G.E.-D.A.E.-R, Turk J. Physics, 27 (2003) 255-262.

[26]. B. R. Judd, Phys. Rev, 127 (1962) 750-761.

[27]. Elias Oliveira Serqueira, Rodrigo Ferreira de Morais, J. Alloys Compounds 560 (2013) 200-207.

[28]. S. Laxmi Srinivasa Rao, Ramadevudu, International J. Engineering. Science and Technology, 4 (2012) 25-35.

[29]. N. H. Bahra, M. S. Jaafar, S.M Iskandar, S. K. Chang, J. Opto electronics & Bio Materials, 7 (2015) 47.

[30]. B. Deva Prasad, C. Madhukar, Optical Materials, 34 (2012) 1251-1260.

[31]. Manisha Pal, Baishakhi Roy, Mrinal Pal, Journal of Modern Physics, 2 (2011) 1062-1066.

[32]. Vikas Dubey, Ratnesh Tiwari, Infrared Physics & Technology, 67 (2014) 537- 541.

[33]. A. A. Alemi, H. Sedghi, A. R. Mirmohseni and V. Golsanamlu, Bull. Material Science, 29 (2006) 55–58.

[34]. A.G. Souza Filho, J. Mendis Filho, F.E.A. Melo, M.C.C. Custodio, R. Lebullenger, A.C. Hernandes, J. Phys. Chem. Solids, 61 (2000) 1535–1542.

[35]. Y. Raja Rao, K. Krishna Murthy Goud, E. Ramesh Kumar, IJRDET, 3 (2014) 122-130.

[36]. L.Baia, R.Stefan, W.Kiefer, J.Popp, S.Simon, J. Non-Cryst. Solids, 303 (2002) 379-386.

[37]. W.T. Carnall, P.R. Fields, K. Rajnak, J. Chem. Phys, 49 (1968) 4424-4442.

[38]. S. Babu, M. Seshadri, V. Reddy Prasad, Y.C. Ratnakaram, Material Research Bulletin, 70 (2015) 935–944.

[39]. L. Pauling, J. American Chemical Society, 51 (1929) 1010-1026.

[40]. A. A. Assadi, K. Damak, R. Lachhed, R. Maalej, J. Alloys Compounds, 620 (2015) 129-136.
[41]. S.F.Ismail, M.R. Sahar, S.K.Ghoshal, J. Materials Characterization, 111 (2016) 177-182.
[42]. A. Amarnath Reddy, S. Surendra Babu, G. Vijaya Prakash, J. Alloys & Compounds, 509 (2011) 4047-4052.
[43]. S. Hima Bindu, T. Rajavardhan, Ch. Linga Raju, Physica Scripta, 90 (2015) 1-9.
[44]. Elias Oliveira Serqueira, Rodrigo Ferreira de Morais, J. Alloys Compounds 560 (2013) 200-207.
[45]. A.S.S.de Camargo, J. F. Possatto, L.A. de .O. Nunes, Solid State Communications 137 (2006) 1-5.
[46]. Y. N. Ch. Ravi Babu, Malathi Rekha, S.V.G.V.A. Prasad, J. Science and Research (2013) 31-35.
[47]. R. Rolli, M. Montagana, S. Chaussedent, V. K. Tikhomirov, Optical Materials 21 (2003) 743-748.
[48]. G. S. Ofelt, Intensites of Crystal spectra of rare earth ions, J. Chemical Physics 37 (1962) 511-520.
[49]. M. V. Vijaya Kumar, K. Ramgopal, B. C. Jalamaiah, J. Luminescence, 142 (2013) 128-134.
[50]. Y. D. Yiannopoulos, G. D. Chryssikos, J. Phys.Chem.Glasses, 42(3) (2001) 164-172.
[51]. P. Babu, Hyo Jin Seo, C. K. Jayasankar, J. Optical Society of America B, 24 (2007) 2218-2228.
[52]. L. R. P. Kassab, L. C. Courrol, R. Seragioli, J. Non-Cryst. Solids, 348 (2004) 94-97.
[53]. S. Suresh, M. Prasad, V. Chandra Mouli, Indian J. Pure & Applied Physics, 47 (2009) 163-169.

Table 1: Chemical composition of present glass matrix

Glass code	M-O ZnO		B_2O_3	Er_2O_3
SZB: Er_1	10	29	60	1
SZB: Er_2	10	28	60	2
SZB: Er_3	10	27	60	3
CZB: Er_1	10	29	60	1
B**ZB: Er_1**	10	29	60	1

Table 2: Physical parameters of the Erbium doped SZB & MZB glasses

Physical parameters (mol %)	**Er^{3+}: SZB 1**	**Er^{3+}: SZB 2**	**Er^{3+}: SZB 3**	**Er^{3+}: CZB 1**	**Er^{3+}: BZB 1**
Density (ρ) (gm / cc)	3.45	3.36	3.25	3.15	3.28
Molar Volume (Vm) (cm^3)	23	24.5	26.3	25.1	27.1
Refractive Index (n)	2.34	2.39	2.43	2.17	2.46
Average molecular weight (gm)	79.5	82.5	85.6	79.2	88.6
Molar refractivity (Rm) cc	13.7	14.9	16.3	13.8	16.9
Conc. Of Er^{3+} ion (10^{20} ions cm^{-3})	2.61	4.91	6.86	2.40	2.22
Polaron radius γp (A^0)	6.3	5.10	4.58	6.48	6.65
Field Strength (10^{14}) cm^{-2}	7.55	11.5	14.3	7.14	6.78
Inter nuclear distance γ_i (A^0)	15.6	12.6	11.3	16.1	16.5
Molar Polarizability αe (10^{-24}) (cm^3)	5.46	5.94	6.47	5.50	6.73
Optical Dielectric constant(ε)	5.47	5.71	5.90	4.71	6.05
Reflection loss (R) %	9.53	10.2	10.4	7.87	10.7
Metallization parameter (M)	0.40	0.39	0.38	0.44	0.37

Table 3: Band gap, Urbach energy, optical basicity of Er^{3+}: SZB & Er^{3+}: MZB glasses

Glass system	Direct band gap (eV)	Indirect band gap (eV)	Urbach energy	Optical basicity
Er_1-SZB	4.04	4.72	0.32	0.635
Er_2-SZB	4.36	4.74	0.38	0.645
Er_3-SZB	4.69	4.76	0.40	0.650
Er_1-CZB	4.14	3.92	0.37	0.631
Er_1-SZB	3.98	4.04	0.32	0.635
Er_1-BZB	4.32	3.80	0.36	0.669

Table 4: Oscillator strength values of the present (Er^{3+}: MZB) glass system

Transition SLJ→S'L'J'	Energy (cm^{-1})	Er_1:SZB		Er_2:SZB		Er_3:SZB		Er_1:CZB		Er_1:BZB	
		f_{exp}	f_{cal}	f_{exp}	f_{cal}	f_{exp}	f_{cal}	f_{exp}	f_{cal}	f_{exp}	f_{cal}
$^4I_{15/2}\rightarrow{}^4G_{9/2}$	27472	5.36	5.19	3.87	2.78	0.980	1.20	2.38	2.51	3.246	1.968
$^4I_{15/2}\rightarrow{}^4G_{11/2}$	26455	46.8	46.2	29.91.	30.02.	14.13	13.3	24.3	24.9	24.93	25.75
$^4I_{15/2}\rightarrow{}^2G_{9/2}$	24630	4.32	4.93	29	01	0.427	0.65	0.12	1.63	1.847	2.172
$^4I_{15/2}\rightarrow{}^4F_{3/2}$	22675	0.72	2.47	0.31	0.98	0.154	0.31	0.41	0.79	0.388	1.103
$^4I_{15/2}\rightarrow{}^4F_{5/2}$	22222	1.75	0.42	1.04	1.69	0.430	0.53	1.03	1.35	0.989	1.89
$^4I_{15/2}\rightarrow{}^4F_{7/2}$	20491	13.4	12.1	4.22	5.12	1.744	1.75	3.47	4.23	3.852	5.21
$^4I_{15/2}\rightarrow{}^2H_{11/2}$	19193	25.4	26.0	17.0	16.9	6.822	7.49	14.8	14.1	15.31	14.5
$^4I_{15/2}\rightarrow{}^4S_{3/2}$	18416	1.87	3.50	0.62	1.39	0.172	0.43	0.45	1.11	0.429	1.55
$^4I_{15/2}\rightarrow{}^4F_{9/2}$	15360	8.71	8.95	4.22	4.43	1.865	1.80	3.38	3.91	3.301	3.54
$^4I_{15/2}\rightarrow{}^4I_{11/2}$	10266	4.57	3.94	1.35	1.68	0.471	0.56	1.07	1.35	1.377	1.82
$^4I_{15/2}\rightarrow{}^4I_{13/2}$	6548	8.56	8.52	3.85	3.51	1.221	1.15	3.14	2.85	4.204	3.78
		δ_{rms} = 0.98 δ = - 0.408 β = 1.041		δ_{rms} = 0.383 δ = -0.404 β = 1.0040		δ_{rms} = 0.117 δ = - 0.378 β = 1.0038		δ_{rms} = 0.434 δ = - 0.244 β = 1.0024		δ_{rms} = 0.722 δ = - 0.209 β = 1.0023	

Table 5: Intensity parameters (Ω_λ x 10^{-20}) using J-O theory

Host matrix	J-O parameters			Trend	$\chi = \Omega_4 / \Omega_6$
	Ω_2	Ω_4	Ω_6		
Er_1-SZB	8.87	1.94	3.78	$\Omega_2 > \Omega_6 > \Omega_4$	0.51 Present work
Er_2-SZB	5.60	1.31	2.82	$\Omega_2 > \Omega_6 > \Omega_4$	0.46 Present work
Er_3-SZB	2.38	0.66	1.69	$\Omega_2 > \Omega_6 > \Omega_4$	0.39 Present work
Er_1-SZB	8.87	1.94	3.78	$\Omega_2 > \Omega_6 > \Omega_4$	0.51 Present work
Er_1-CZB	5.48	1.54	1.75	$\Omega_2 > \Omega_6 > \Omega_4$	0.88 Present work
Er_1-BZB	4.81	0.51	1.93	$\Omega_2 > \Omega_6 > \Omega_4$	0.40 Present work
Silicate Glass	4.20	1.85	1.62	$\Omega_2 > \Omega_6 > \Omega_4$	1.11 [08]
Phosphate glass	8.05	1.46	2.28	$\Omega_2 > \Omega_6 > \Omega_4$	0.64 [08]
Lead	5.89	1.85	2.50	$\Omega_2 > \Omega_6 > \Omega_4$	0.74 [46]
PTB-Er	5.69	0.31	1.74	$\Omega_2 > \Omega_6 > \Omega_4$	0.17 [47]

Table 6: Amplification parameters of $^4I_{13/2}\rightarrow{}^4I_{15/2}$ transition of Er^{+3} ions

Host System	A_R (s^{-1})	β_R	τ_R (ms)	τ_m (ms)	ɲ (%)
Er_1-SZB	239	1	4.18	1.77	42
Er_2-SZB	243	1	4.11	1.71	42
Er_3-SZB	248	1	4.02	1.65	41
Er_1-CZB	254	1	3.9	1.08	28
Er_1-SZB	239	1	4.18	1.77	42
Er_1-BZB	228	1	4.41	2.03	46
PKSAEr10 *[02]*	*134*	*1*	*7.43*	*0.87*	*12*
Tellurite glass *[24]*	*334*	*1*	*2.98*	*0.20*	*07*
Er:NAP *[42]*	*----*	*---*	*9.16*	*3.97*	*43*

Table 7: Effective line width, $\Delta\lambda_{eff}$ (nm), emission cross-section, σ_e (cm^2), gain bandwidth, ΔG (cm^2) of $^4I_{13/2} \rightarrow {}^4I_{15/2}$ transition of various Er^{3+}:MZB glasses.

Host composition	$\Delta\lambda_{eff}$ (nm)	σ_e (10^{-21} cm^2)	ΔG (10^{-28} cm^2)
Er_1-SZB	69	3.7	138
Er_2-SZB	72	4.3	197
Er_3-SZB	73	5.3	292
Er_1-SZB	69	3.7	138
Er_1-CZB	56	4.9	185
Er_1-BZB	49	3.0	99
Phosphate [36]	37	6.4	237
Germinate [38]	53	5.6	301
Silicate [53]	45	5.5	396

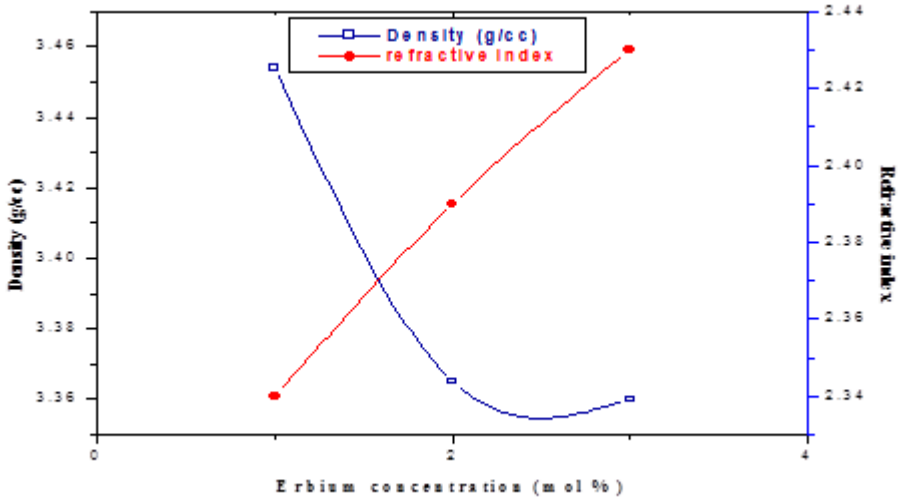

Fig.1: The variation of density with refractive index as a function Er^{3+} ion concentration.

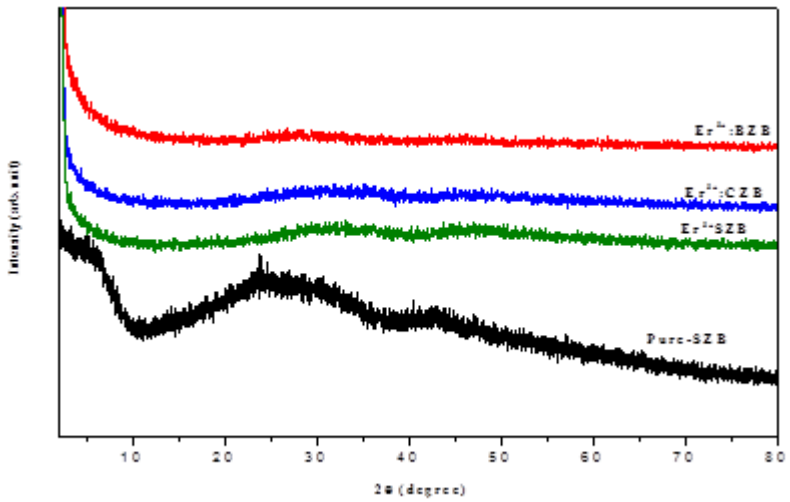

***Fig.2:** XRD pattern of pure and doped Er^{3+}: MZB glass.*

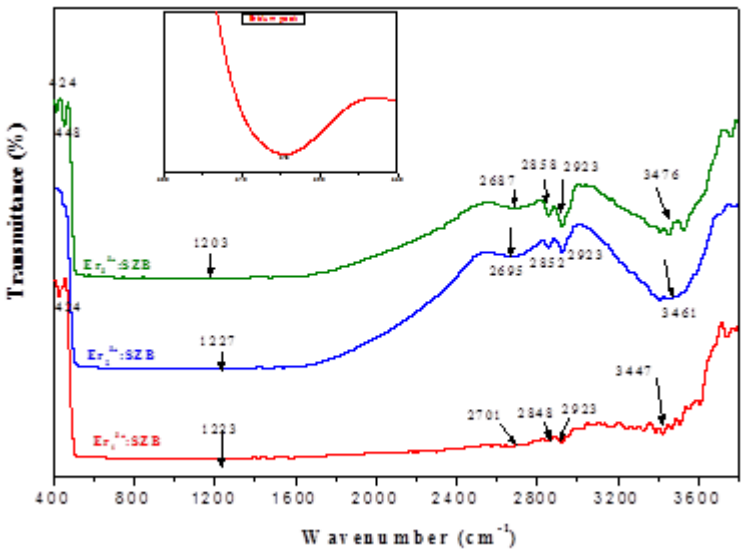

Fig.3 (a): *FT-IR spectra of erbium doped SZB glasses.*

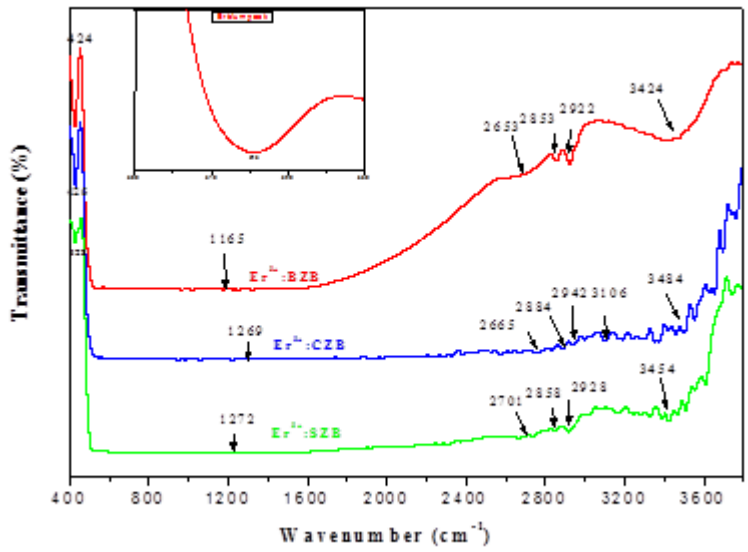

Fig.3 (b): *FT-IR spectra of erbium doped MZB glasses.*

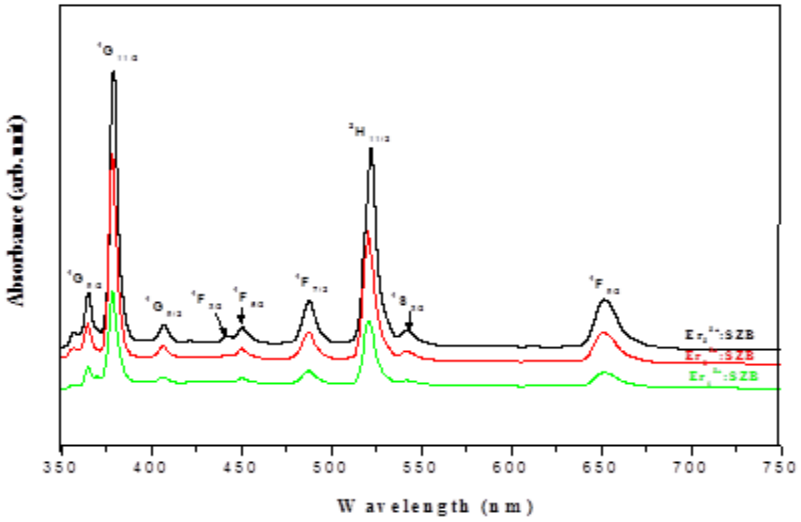

(a)

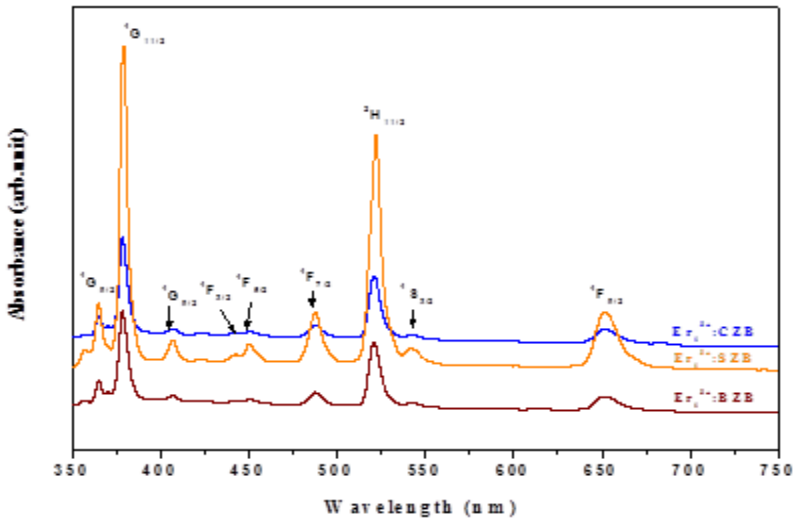

Fig.4 (a): Optical absorption spectra of Er^{3+}: SZB & Er^{3+}: MZB glasses in UV-VIS region.

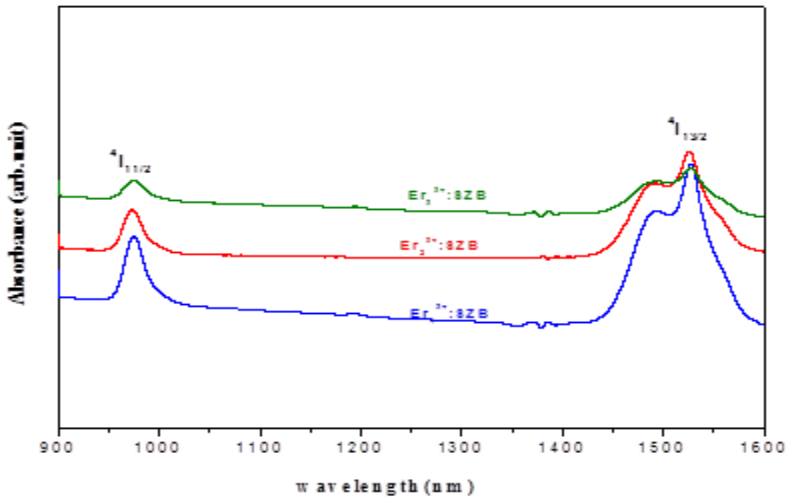

(b)

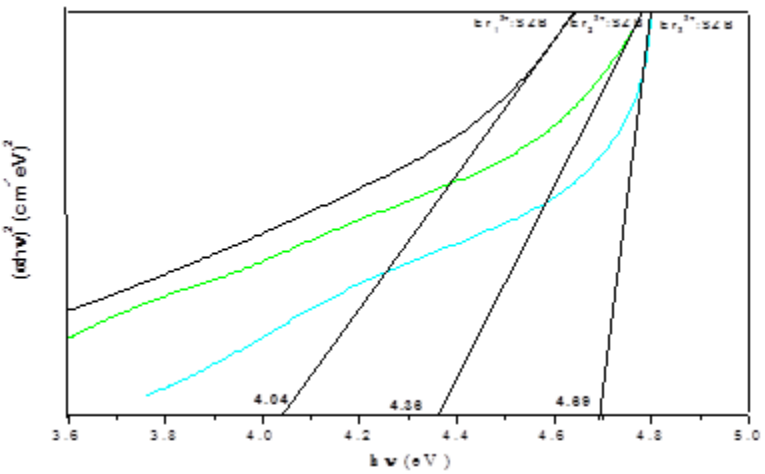

Fig.4 (b): Optical absorption spectra of Er^{3+}: SZB & Er^{3+}: MZB glasses in NIR region.

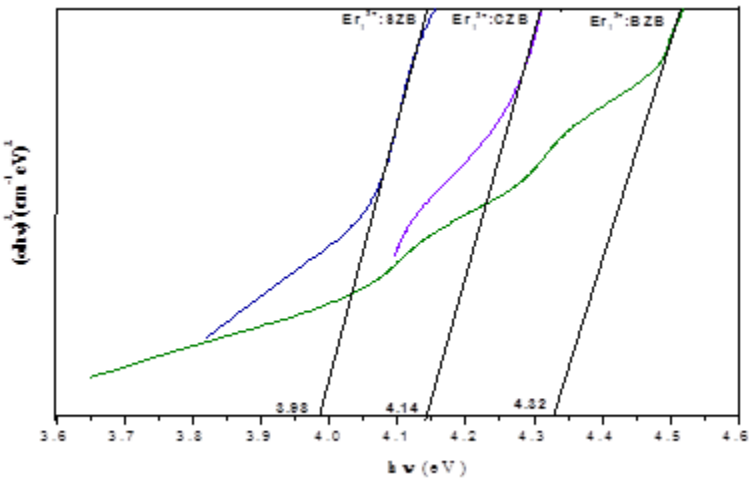

(a)

Fig.5 (a): The Tauc's plots of $(\alpha h\upsilon)^2$ vs hu for Er^{3+}: SZB and Er^{3+}: MZB glasses.

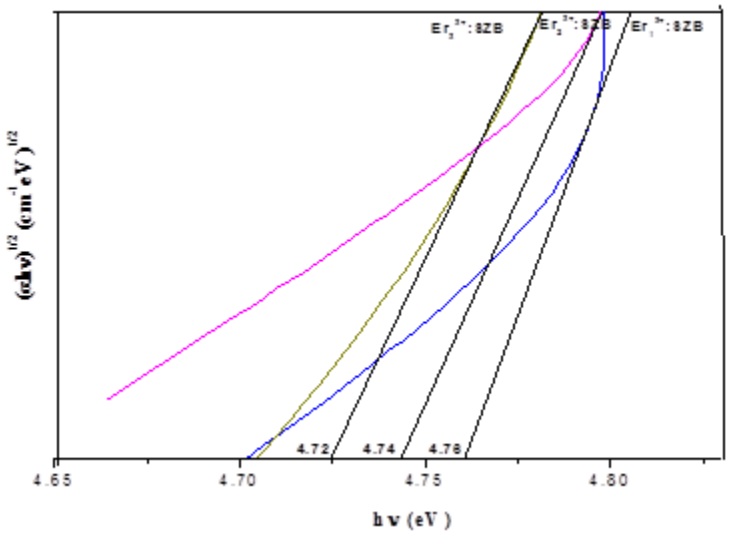

(b)

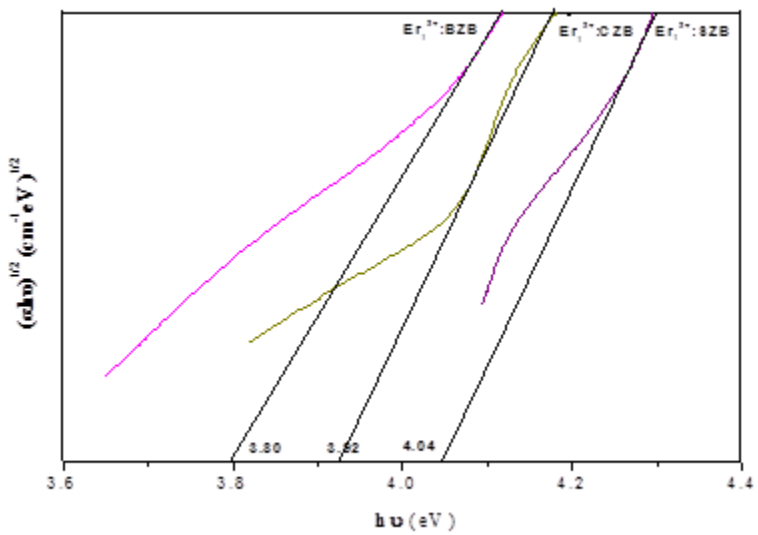

Fig.5 (b): The Tauc's plots of $(\alpha h\upsilon)^{1/2}$ vs hu for Er^{3+}:SZB and Er^{3+}: MZB glasses.

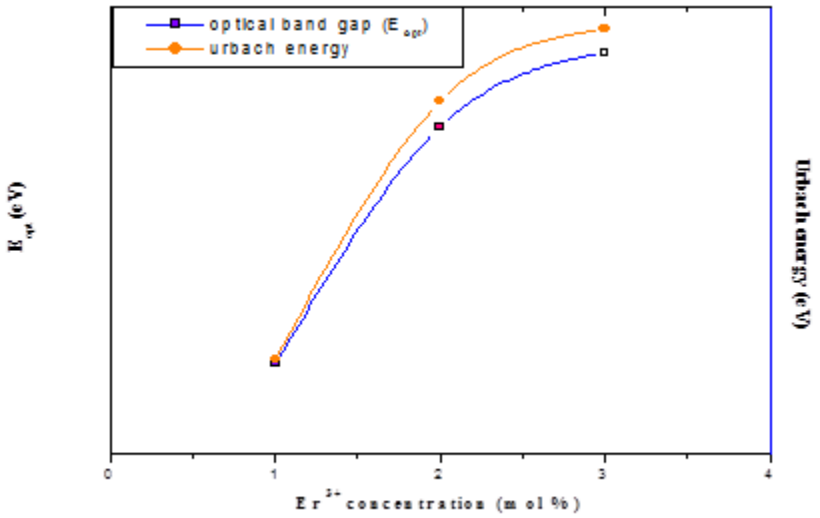

Fig.6 (a): The variation of optical band gap and Urbach energy with dopant concentration.

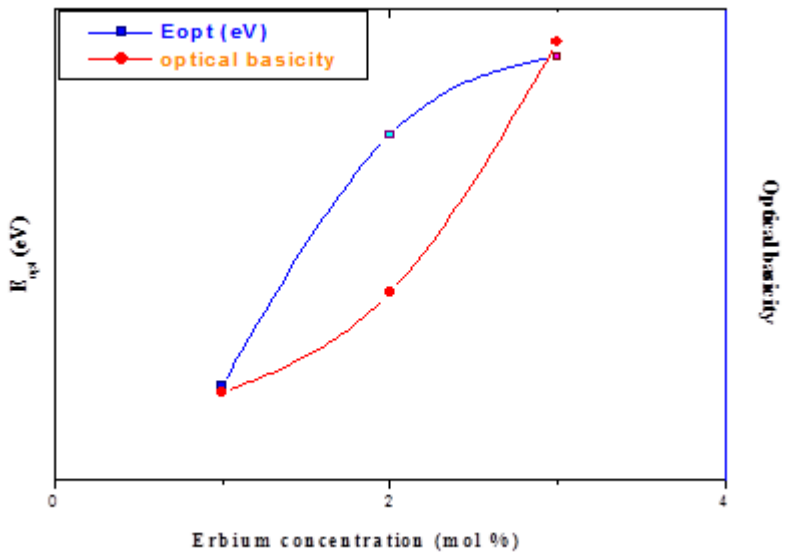

Fig.6 (b): The variation of optical band gap and optical basicity with dopant concentration.

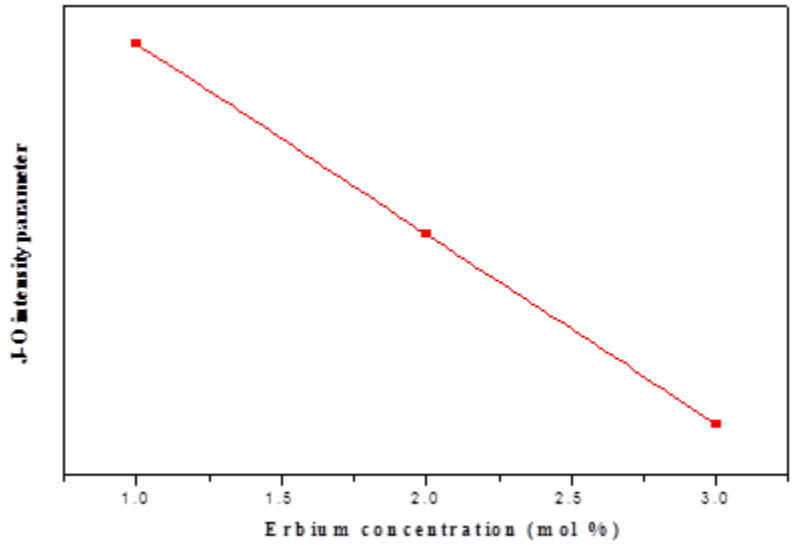

Fig.7: The variation of J-O parameter with erbium ion concentration.

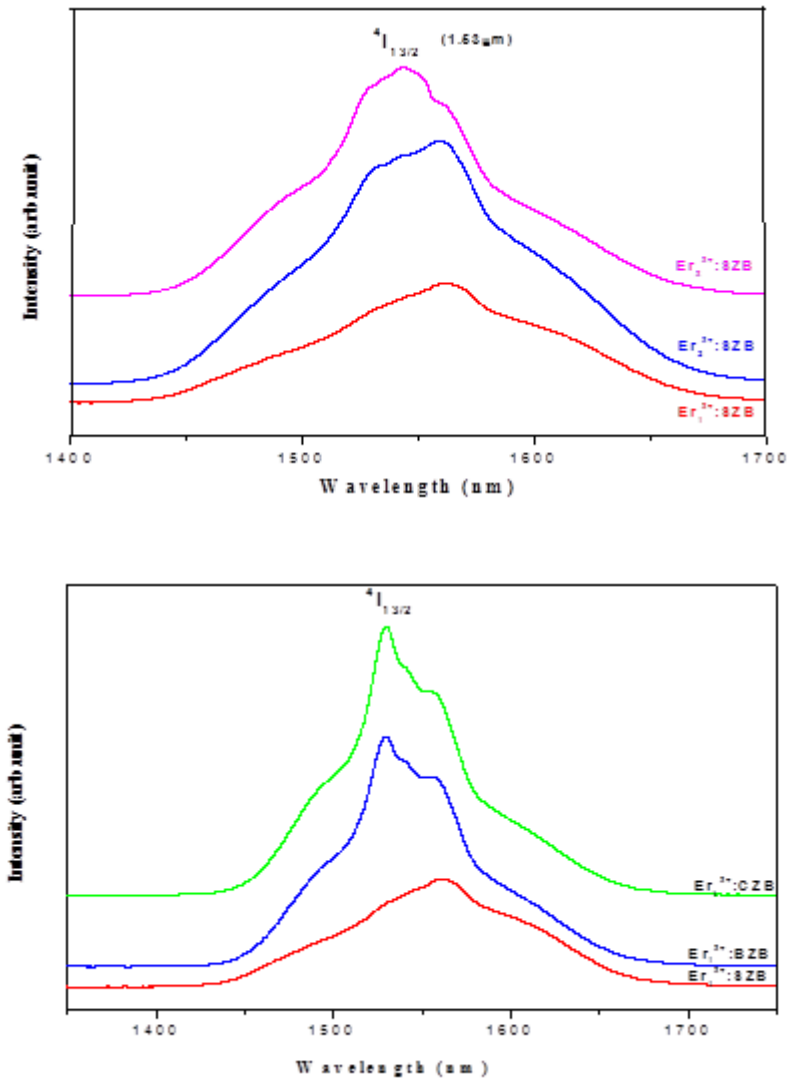

Fig.8: Fluorescence emission spectrum of $^4I_{13/2} \rightarrow {}^4I_{15/2}$ transition in Er^{3+}: SZB and Er^{3+}: MZB glasses.

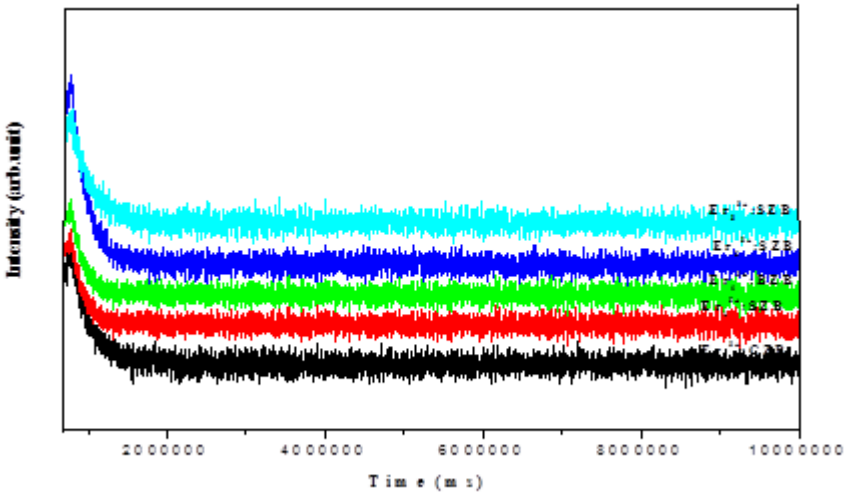

Fig.9: Decay curves for $^4I_{13/2}$ level of Er^{3+}: MZB glass.